ADVANCES IN ATMOSPHERIC SCIENCES, VOL. 37, MAY 2020, 545–554

• **Original Paper** •

Refractory Black Carbon Results and a Method Comparison between Solid-state Cutting and Continuous Melting Sampling of a West Antarctic Snow and Firn Core

Luciano MARQUETTO*[1,2], Susan KASPARI[1], Jefferson Cardia SIMÕES[2], and Emil BABIK[1]

[1]*Department of Geological Sciences, Central Washington University, Ellensburg, Washington* 98926, *USA*

[2]*Polar and Climatic Center, Federal University of Rio Grande do Sul, Porto Alegre, Rio Grande do Sul*, 91509-900, *Brazil*

(Received 12 July 2019; revised 4 September 2019; accepted 24 October 2019)

ABSTRACT

This work presents the refractory black carbon (rBC) results of a snow and firn core drilled in West Antarctica (79°55'34.6"S, 94°21'13.3"W) during the 2014–15 austral summer, collected by Brazilian researchers as part of the First Brazilian West Antarctic Ice Sheet Traverse. The core was drilled to a depth of 20 m, and we present the results of the first 8 m by comparing two subsampling methods—solid-state cutting and continuous melting—both with discrete sampling. The core was analyzed at the Department of Geological Sciences, Central Washington University (CWU), WA, USA, using a single particle soot photometer (SP2) coupled to a CETAC Marin-5 nebulizer. The continuous melting system was recently assembled at CWU and these are its first results. We also present experimental results regarding SP2 reproducibility, indicating that sample concentration has a greater influence than the analysis time on the reproducibility for low rBC concentrations, like those found in the Antarctic core. Dating was carried out using mainly the rBC variation and sulfur, sodium and strontium as secondary parameters, giving the core 17 years (1998–2014). The data show a well-defined seasonality of rBC concentrations for these first meters, with geometric mean summer/fall concentrations of 0.016 μg L^{-1} and geometric mean winter/spring concentrations of 0.063 μg L^{-1}. The annual rBC concentration geometric mean was 0.029 μg L^{-1} (the lowest of all rBC cores in Antarctica referenced in this work), while the annual rBC flux was 6.1 μg m^{-2} yr^{-1} (the lowest flux in West Antarctica records so far).

Key words: black carbon, West Antarctica, ice core, single particle soot photometer

Citation: Marquetto, L., S. Kaspari, J. C. Simões, and E. Babik, 2020: Refractory black carbon results and a method comparison between solid-state cutting and continuous melting sampling of a West Antarctic snow and firn core. *Adv. Atmos. Sci.*, **37**(5), 545–554, https://doi.org/10.1007/s00376-019-9124-8.

Article Highlights:

- The continuous melting system with discrete sampling is a faster and reliable way of analyzing low rBC concentration samples.
- The record showed a well-defined seasonal signal for black carbon, with higher concentrations during the Southern Hemisphere dry season.
- The sample concentration influences the analysis reproducibility more than the analysis time.
- The annual black carbon concentration was lower than other West Antarctic records and comparable to high-elevation East Antarctica ice cores.

1. Introduction

Black carbon (BC) is a carbonaceous aerosol formed during the incomplete combustion of biomass and fossil fuels, characterized by strong absorption of visible light and resistance to chemical transformation (Petzold et al., 2013). Increases in BC concentrations since the industrial revolution have been observed in ice sheets and caps around the world, with direct implications for the planetary albedo (Hansen and Nazarenko, 2004; Bice et al., 2009; Bond et al., 2013).

Approximately 80% of Southern Hemisphere BC emissions are from in-situ biomass burning, mainly from forest and savannah deforestation (Bice et al., 2009), with 80%–95% of this burning being human-related (Lauk and Erb, 2009). Ice cores retrieved from the Antarctic continent record these Southern Hemisphere emissions and long-

* Corresponding author: Luciano MARQUETTO
Email: luciano.marquetto@gmail.com

© Institute of Atmospheric Physics/Chinese Academy of Sciences, and Science Press and Springer-Verlag GmbH Germany, part of Springer Nature 2020

range transport of BC from low- and midlatitudes (Bisiaux et al., 2012a, b). Long-range transport of BC from low- and midlatitudes to the polar ice caps is possible due to BC's insolubility, graphite-like structure and small size (< 10 nm to 50 nm diameter), resulting in low chemical reactivity in the atmosphere and slow removal by clouds and precipitation unless coated with water-soluble compounds (Petzold et al., 2013). BC concentrations in Antarctica have already been linked to biomass burning from South America, Africa and Australia (Koch et al., 2007; Stohl and Sodemann, 2010; Arienzo et al., 2017). Although there are records of Southern Hemisphere paleo-biomass burning (Marlon et al., 2008, 2016; Wang et al., 2010; Osmont et al., 2018a), there are only a few recent publications on BC variability in ice cores from Antarctica (Bisiaux et al., 2012a, b; Arienzo et al., 2017). More ice core records from different time scales are needed to understand the spatial variability of BC transport to, and deposition in, Antarctica, as well as to improve general circulation models (Bisiaux et al., 2012b).

This work discusses two subsampling methods [solid-state cutting (SSC) and a continuous melting system (CMS)], and the system setup, used to analyze refractory black carbon (rBC) in the first eight sections of a snow and firn core collected in West Antarctica. A preliminary environmental interpretation is also presented.

2. Site description and field campaign

The core was drilled on the Pine Island Glacier at (79°55'34.6"S, 94°21'13.3"W; elevation: 2122 MSL), near the Mount Johns Nunatak (located 70 km northeast of the drilling site) where the ice thickness is 2400 ± 300 m (Fretwell et al., 2013) (Fig. 1). The majority of air masses arrive from the Amundsen Sea and, secondarily, from across the Antarctic Peninsula and Weddell Sea (Schwanck et al., 2017). As stated by Schwanck et al. (2016b), the site was chosen due to (1) its relatively high accumulation rate (0.21 water equivalent meters per year); (2) it is a drainage basin divide (between the Pine Island and Institute Glacier); and (3) it is an area where air masses from the Weddell, Amundsen and Bellingshausen seas converge. It is located approximately 350 km from the West Antarctic Ice Sheet (WAIS) Divide drilling site, from where Bisiaux et al. (2012b) recovered the first, and until now, only high-temporal-resolution rBC record from West Antarctica covering recent decades.

The drilling was part of the First Brazilian West Antarctic Ice Sheet Traverse, carried out in the austral summer of 2014–15 along a 1440-km route from Union Glacier (79°46′05″S, 83°15′42″W) in the Ellsworth Mountains, to the automated Brazilian atmospheric module Criosfera 1 (84°00'S, 79°30'W), and then to the Mount Johns area (79°55'34.6"S, 94°21'13.3"W). We used a Mark III auger (Kovacs Enterprises, Inc., Roseburg, OR, USA) coupled with an electrical drive powered by a generator (kept downwind at a minimum of 30 m away) to retrieve all cores in the traverse. The core presented in this study (TT07) was drilled from the surface to a total depth of 20.16 m, divided in 21 sections of less than 1 m each. The borehole temperature was −34°C, measured at 12 m deep by a probe previously calibrated that remained in the borehole for at least 8 h.

All sections of the core were weighed in the field, packed in polyethylene bags and then stored in high-density styrofoam boxes. These boxes were sent by air to Punta Arenas (Chile), then to a deposit in Bangor (USA) for storage, and finally to the Central Washington University (CWU) Ice Core Laboratory (Ellensburg, WA), where it was kept at −18°C in a clean, cold room until subsampling and analysis.

3. Materials and methods

3.1. *rBC analysis in snow and ice samples*

We used an extended range single particle soot photometer (SP2, Droplet Measurement Technologies, Boulder, CO, USA) to analyze the core, and thereby our results are measurements of rBC (Petzold et al., 2013). The particle size range detected by the SP2 at CWU was 80–2000 nm (mass-equivalent diameter) for the incandescent signal, assuming a void-free BC density of 1.8 g cm^{-3} (Moteki and Kondo, 2010).

The SP2 was initially designed to measure rBC in the atmosphere, and then adapted to analyze snow and ice samples. It was first used by McConnell et al. (2007) to analyze an ice core retrieved from Greenland spanning 1788–2000 AD, and since then the method has been applied in numerous studies (Kaspari et al., 2011; Bisiaux et al., 2012a, b; Kaspari et al., 2014, 2015; Casey et al., 2017; Osmont et al., 2018a, b; Sigl et al., 2018). As the system was designed to analyze airborne samples, it is necessary to add an aerosolization step in order to analyze the snow and

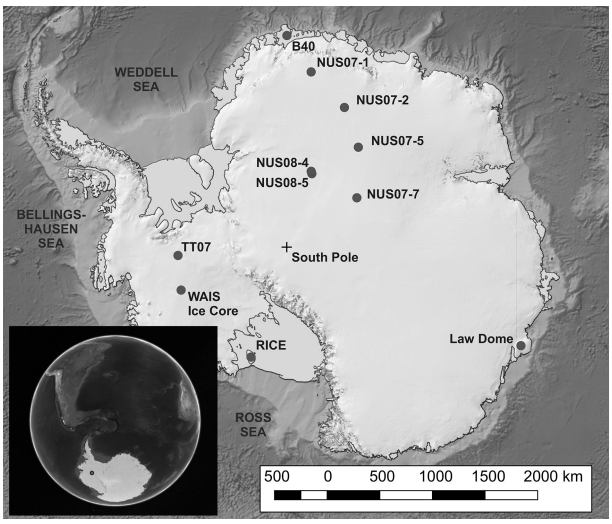

Fig. 1. Drilling location for the snow and firn core analyzed in this work (TT07) and other BC cores mentioned in the text. The bottom-left inset shows the drilling site in perspective to South America. Base map from the Quantarctica Project (Matsuoka et al., 2018).

ice meltwater (Wendl et al., 2014).

For the SP2 external calibration (Wendl et al., 2014), five fresh standards ranging from 0.01 to 1.0 μg L^{-1} were prepared every day in glass jars, by diluting a 4585.6 μg L^{-1} Aquadag stock in Milli-Q water (MilliQ-Element, Millipore, Milford, USA, 18.2 MΩ cm) previously sonicated for 15 min. Aquadag (Acheson Industries Inc., Port Huron, MI, USA) is an industrial, graphite-based lubricant consisting of a colloidal suspension of aggregates of graphitic carbon in water, with a content of BC between 71% and 76% of solid mass, proven suitable for calibration standards by Wendl et al. (2014).

An environmental standard (diluted meltwater of a snow sample from Table Mountain, WY, USA) of known concentration (0.18 ± 0.04 μg L^{-1}) was also analyzed every day, to ensure there were no mistakes when preparing the Aquadag standards. The Aquadag stock and the environmental standard were kept in closed glass jars and refrigerated at ~5°C when not in use, and sonicated for 15 min prior to usage. For the nebulization step we used a CETAC Marin-5, described by Mori et al. (2016).

Internal calibration of the SP2 (Wendl et al., 2014) was carried out using a known polydisperse BC standard of aqueous Aquadag diluted in Milli-Q water. The Aquadag solution was nebulized, and then passed through a sillica diffusion drier (to remove moisture) and an x-ray source (Advanced Aerosol Neutralizer Model 3088, TSI Inc., MN, USA) to neutralize particle charges before entering a centrifugal particle mass analyzer (CPMA), similar to the set up in Olfert et al. (2007) but without the differential mobility analyzer. The CPMA was configured to select 23 particle masses from 0.5 fg to 800 fg. Each selected mass ran for 30 min to 6 h to provide statistically significant particle triggers to calibrate the SP2, and calibration curves were then generated for all SP2 channels. The data presented here are from the duplicated extended range broadband detector, as this channel gave the best-fit calibration curve of all channels, with a precise fitting in the lower end of the particle mass range. For more details on the calibration, see Table S1 and Fig. S1 in the electronic supplementary material (ESM).

3.2. *Sample preparation*

The sample preparation process consisted of removing the outer layers of the core, as these are prone to contamination during drilling, handling and transport of the core (Tao et al., 2001). Antarctic samples are especially sensitive to contamination owing to the very low concentrations of analytes commonly observed in them. Previous works have shown rBC concentrations in West Antarctic snow to be as low as 0.01 μg L^{-1} (Bisiaux et al., 2012b). Regular, intensive cleaning was carried out inside the cold room for all surfaces/parts/equipment in contact with the core using ethanol and laboratory-grade paper tissues. Tyvek suits (DuPont, Wilmington, DE, USA) and sterile plastic gloves were used at all times in the cold room during the core processing. Vials used to store the samples (50-mL polypropylene vials) were soaked in Milli-Q water for 24 h and rinsed three times. This process was repeated two more times, in a total of three days soaked in Milli-Q water and nine rinses. The vials were left to dry, covered from direct contact, in the laboratory.

We used two different methods to analyze the core in order to compare them: SSC and a CMS. We partitioned the 21 sections of the core longitudinally, using a bandsaw with a meat grade, stainless steel bandsaw blade, and samples from the same depths were prepared using SSC and the CMS (the cut plan is presented in Fig. S2 in ESM). For every cutting session, a Milli-Q ice stick, previously prepared, was cut in the beginning, to guarantee a clean blade for the snow and firn core. For both methods, we hand-scraped the resulting snow and firn sticks with a clean ceramic knife, to remove the outer snow/firn layer (2–4 mm). This process was carried out in a laminar flow hood, still in the cold room.

3.2.1. *SSC*

The SSC method consisted of cutting the hand-scraped snow and firn sticks in 2–2.5-cm samples with a ceramic knife, resulting in ~40 samples (of 6–8 mL each) per section. This process was also carried out in the laminar flow hood. We stored the samples in pre-cleaned 50-mL polypropylene vials and kept them frozen until analysis.

Samples were melted at room temperature or in a tepid bath not exceeding 25°C, sonicated for 15 min, and then analyzed (in less than 1 h after melting).

3.2.2. *The CMS*

We assembled a CMS at the CWU Ice Core Laboratory, based on the system developed at the Climate Change Institute (CCI), University of Maine, USA—described in detail in Osterberg et al. (2006) and used by Schwanck et al. (2016a, b, 2017). The main advantage of the CMS compared to SSC is the reduced handling of samples.

The inner part of the core was collected with a fraction collector in pre-cleaned 50-mL polypropylene vials for rBC analysis, resulting in ~43 samples (of 6–10 mL each) per section. The outer part of the core was discarded. The samples were kept refrigerated at 5°C until the time of analysis, and were then sonicated for 15 min and analyzed (less than 2 h after melting). As the flow remained constant, the sample depth was calculated by dividing the length of each section by the number of resulting samples.

The main differences between the melting system used at CCI and the one assembled at CWU are:

(1) The system was built to only collect samples for rBC, meaning we only collect the melting water from the inside ring of the melting head. This also means we only use two peristaltic pumps—one for the inside ring and another for the outside ring (wastewater).

(2) The melting disk at CWU is made of aluminum (not nickel); as we are not analyzing samples for heavy metals, there is no need for a high-purity nickel disk.

(3) As samples are less prone to BC contamination in

comparison to trace-element contamination, the fraction collector linked to the melting system sits on a normal lab bench, not in a flow hood.

(4) The melting head temperature during use is set to 10°C–15°C (instead of 15°C–20°C as commonly used at CCI). Higher temperatures generate persistent wicking processes, and this lower temperature range causes less of a problem (although wicking never stops completely). Due to time constraints related to the assembling and testing of the continuous melter, we could only prepare and analyze eight sections with this method.

3.3. *Whole-system setup*

After melting, the sample is dispensed to the Marin-5 nebulizer by a Regro Digital peristaltic pump (ISMATEC, Wertheim, Germany) at 0.14 ± 0.02 mL min^{-1} and monitored by a TruFlo Sample Monitor (Glass Expansion, Port Melbourne, Australia). The Marin-5 nebulizer receives standard laboratory air at 1000 sccm (1.000 L min^{-1}), regulated by an Alicat Flow Controller (Alicat Scientific, Tucson, AZ, USA) connected to a Drierite Gas Purifier, which removes any moisture or particulates from the air. The nebulizer heating and cooling temperatures are set to 110°C and 5°C, respectively, following Mori et al. (2016). We used Tygon Long Flex Life (LFL) tubing ID 1.02 mm (Saint-Gobain Performance Plastics, France) for sample to nebulizer connection.

The SP2 flow was maintained at 120 volumetric cm^3 min^{-1} (vccm). YAG laser power for this project stayed constant above 5.0 V.

Procedural blanks (MQ water) were run at the beginning and end of every working day, and also every 15–20 samples. Background levels were kept at 0–0.5 particles cm^{-3} and a 5% nitric acid solution was used for cleaning the tubing and nebulizer when needed. For the SP2 to return to background levels, only MQ water was used. Peristaltic pump tubing replacement was necessary only once during the process.

The limit of detection (LOD) of the method was estimated to be 1.61×10^{-3} µg L^{-1}, based on procedural blanks measured to characterize the instrument detection limit (mean + 3σ, $n = 30$).

Samples were analyzed for 5 min each, with a whole-system reproducibility test carried out to assess the uncertainty related to the method. This test is presented in section 4.4.

Data processing was performed with the SP2 Toolkit 4.200 developed by the Laboratory of Atmospheric Chemistry at the Paul Scherer Institute, and was used on the IGOR Pro version 6.3 scientific data analysis software.

3.4. *Fire-spots database*

To help define the dating of the core, we compared our rBC results with fire spots (number of active fires) detected by satellites for the Sentinel Hotspots program (Geoscience Australia, Australia, available at https://sentinel.ga.gov.au/) and Programa Queimadas (Instituto Nacional de Pesquisas Espaciais, Brazil, available at http://www.inpe.br/queimadas/portal). Both systems use the MODIS, AVHRR and VIIRS sensors to pinpoint fire spots. Sentinel Hotspots presents data from 2002 to present and covers Australia and New Zealand, while Programa Queimadas has data from 1998 to present, and covers all South American countries.

Although Africa has the highest total BC emissions of the Southern Hemisphere, the continent contributes little to BC in Antarctica because emissions are located further north than South American and Australian emissions (Stohl and Sodemann, 2010).

Even though the parameter "fire spot" used in both Australian and Brazilian fire monitoring programs does not translate directly to the dimension and intensity of the biomass burning events, it holds a correlation with burned area (Andela et al., 2017), and so we consider it useful to our comparison.

3.5. *rBC concentrations and fluxes*

The frequency distributions of the TT07 core rBC concentrations were determined to be lognormal, and so we present geometric means and geometric standard deviations because these are more appropriate than arithmetic calculations (Limpert et al., 2001; Bisiaux et al., 2012a). Note that the geometric standard deviation is the multiplicative standard deviation (σ^*), so the 68.3% confidence interval is calculated as σmin_{conc} = geometric mean × geometric standard deviation, and σmax_{conc} = geometric mean / geometric standard deviation (Limpert et al., 2001).

We present our data as summer/fall (dry season) concentrations and winter/spring (wet season) concentrations. Wet/dry season concentrations and annual concentration geometric means and standard deviations were calculated in the raw rBC measurements using the dating carried out to separate years and rBC concentration variations to pinpoint the changes from dry season to wet season, and vice versa. Monthly mean concentrations were calculated by applying a linear interpolation in the raw measurements.

rBC fluxes were calculated by multiplying annual rBC means by annual snow accumulation. Annual snow accumulation was estimated based on our field measurements and the density profile from another 45-m-deep core drilled in the same area studied by Schwanck et al. (2016b) (described in section 4.1).

4. Results and discussion

4.1. *Core description*

During transport between Antarctica and the University of Maine the core was exposed to above-freezing temperatures and some sections were partially melted and refrozen. As the core was transported lying down in the boxes, this melt and refreeze occurred in the external part of the core and did not reach the center of it. The melted and refrozen portion of the core was removed by saw and hand scraping, and only a small 10-cm piece of section 07 was discarded as it was totally refrozen.

We used an ice core light table to observe the core stratigraphy. Millimeter-thick lenses of ice were observed all along the core, probably due to summer melting. Additionally, a few depth hoar layers up to 1 cm thick were observed. There were no visible dust layers.

The core density ranged from 0.38 to 0.60 g cm^{-3}, not reaching the firn/ice transition of 0.83 g cm^{-3} (Fig. 2). We averaged the TT07 density profile with the density profile of another core drilled in the same area of Antarctica (45 m deep; Schwanck et al., 2016b), fitted a quadratic trend line to the average curve, and used this trend line to calculate the snow accumulation, water equivalent (weq), and rBC fluxes for this work. We found an average snow accumulation of 0.23 ± 0.06 weq m yr^{-1} for the entire core, so the 20.16-m length core represents 10.65 weq m. For the 8 m analyzed in this work, the snow accumulation was 0.21 ± 0.04 weq m.

4.2. *Dating*

The first eight sections of the core, presented in this work, were dated to 17 years by annual-layer counting using mainly the rBC seasonal variability, as this is a reliable parameter for dating (Winstrup et al., 2017). Data from Sentinel Hotspots indicate fires in Australia tend to peak in October, with the seasonal increase in fire activity occurring in August and the decrease in December/January. The Programa Queimadas data show that fires in South America tend to peak in September, with the seasonal increase in fire activity occurring in June/July and the decrease in November/December. A comparison between the seasonality of burning and the TT07 rBC record is presented in Fig. S3 in ESM.

As a support to this, we used sulfur (S), strontium (Sr) and sodium (Na), as these records show the more pronounced seasonal variability at the site (Schwanck et al., 2017), although we only had these analyzed down to ~7 m of the core. Also, the S, Sr and Na records are from a different core, retrieved a meter apart from the rBC core, and that core was subsampled and analyzed in another laboratory (CCI), meaning there could be some displacement from this record to the rBC one. The dating is presented in Fig. 3.

BC in Antarctica tends to peak during winter–spring (dry season) owing to drier conditions in the Southern Hemisphere and a consequent increase in biomass burning (Bisiaux et al., 2012b; Sand et al., 2017; Winstrup et al., 2017). Na and Sr also peak during this time, due to intense atmospheric circulation and transport (Legrand and Mayewski, 1997), while S peaks in late austral summer in relation to marine biogenic activity (Schwanck et al., 2017). We considered our new year to match the end of what we define as

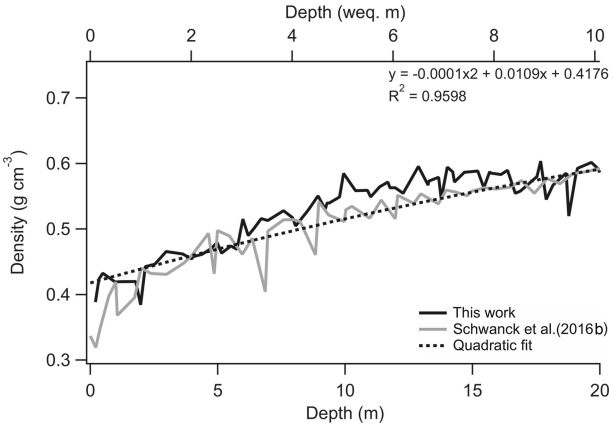

Fig. 2. Density profile of the snow and firn core analyzed. Depth is presented in meters and water equivalent (weq) meters. The quadratic fit was calculated from the average density profile from this work and from Schwanck et al. (2016b).

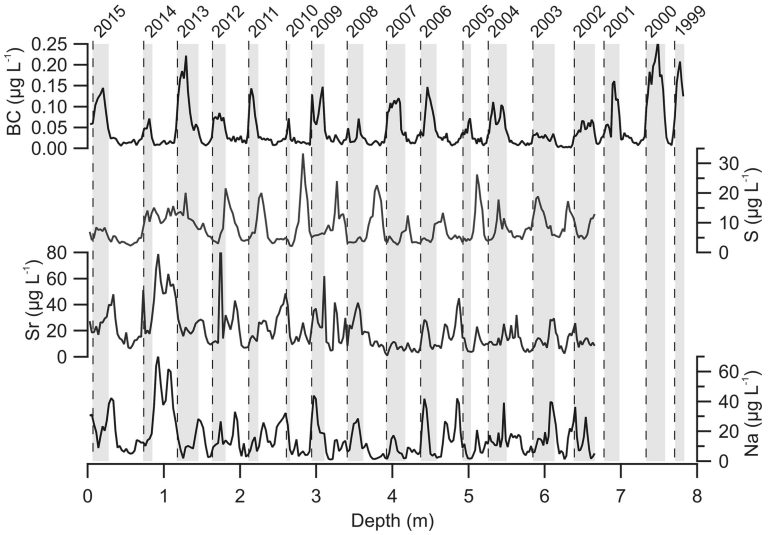

Fig. 3. Dating of the snow and firn core based on BC, S, Sr and Na records. Dashed lines indicate the estimated New Year. In this figure, we present the BC record from the CMS, as this was smoother than that from SSC. Gray shaded areas are the dry-season (winter/spring) concentrations, while white areas are the wet-season (summer/fall) concentrations.

the dry season, as this is a reliable tying point in the record because of the abrupt drop in rBC concentrations based on the fire-spot database from Australia and South America. This is also in agreement with Winstrup et al. (2017), who stated that rBC tends to peak a little earlier than New Year in their records (Roosevelt Island Ice Core).

4.3. *Nebulization efficiency*

The nebulization efficiency for the Marin-5 at CWU was calculated to be 68.31% ± 5.91% (1σ), based on external calibration carried out every working day using the Aquadag standards (see section 3.1). We found a decrease in nebulization efficiency during the laboratory work period (−0.31% per working day or −13.3% over the 43 working days), but we assume the nebulization efficiency to have remained stable between the measurement of the standard and the samples measured for the day, as in Katich et al. (2017). We attribute this decrease to the Marin-5, but do not see any apparent cause. Pump flow rates were kept constant at 0.14 ± 0.02 mL min^{-1} at all times during analysis. This result highlights the importance of making daily Aquadag standards.

4.4. *Whole-system repeatability*

Samples were analyzed for 5 min each. Although a low particle count could increase the uncertainty of the method, we noticed that the measurements did not vary significantly in relation to analysis time, but much more so in relation to the sample average concentration itself.

To address this issue, we analyzed samples of varied rBC concentrations along the entire core more than once and for different periods of time. Each sample was analyzed between two and four times, for 5, 20 and/or 40 min. The samples were analyzed less than 2 h after melting to avoid rBC loss (Wendl et al., 2014).

While we observed no significant concentration variations for different analysis times (Fig. 4), our coefficient of variation (mean of all measurements of the sample × standard deviation) for concentrations lower than 0.03 μg L^{-1} was 25.7 ± 16.9 (1σ, n = 38), 10.4 ± 6.6 (1σ, n = 24) for concentrations between 0.03 and 0.07 μg L^{-1}, and 7.3 ± 4.4 (1σ, n = 51) for concentrations higher than 0.07 μg L^{-1} (Fig. 5).

We attribute this variation to the number of collected particles in each sample: low-concentration samples mean low particle triggers, which will lead to a higher variance in case rare particles large enough to contain a considerable fraction of total rBC mass are recorded.

4.5. *rBC concentrations and fluxes*

We found a well-marked seasonal rBC cycle along the core (Fig. 6), with the same pattern of low summer/fall and high winter/spring concentrations as reported by Bisiaux et al. (2012b).

As we collected our samples in January and the drilling was carried out from the snow surface, our core starts approximately in the New Year. As mentioned earlier, BC in Antarctica tends to peak during winter/spring, and so the New Year in the record is generally viewed as a steep decrease from peak concentrations to low concentrations. This was better observed in the CMS samples than the SSC ones for the 2014–15 transition.

Both sampling methods showed similar seasonality, but the CMS provided a smoother record (e.g., less summer/fall spikes) and a generally lower summer/fall concentration. Table 1 presents the details of this comparison. We attribute the smoother record to reduced handling of the core, as with SSC the individual samples were handled after decontamination to put them in the clean vials, which could have caused cross-contamination between samples to some degree. Nonetheless, a Wilcoxon–Mann–Whitney test indicated there to be no statistical difference between the two sample datasets at p = 0.01 (N = 650; two-tailed P-value = 0.449758; see Methods S1 in ESM).

For SSC, concentrations ranged from 0.003 μg L^{-1} to

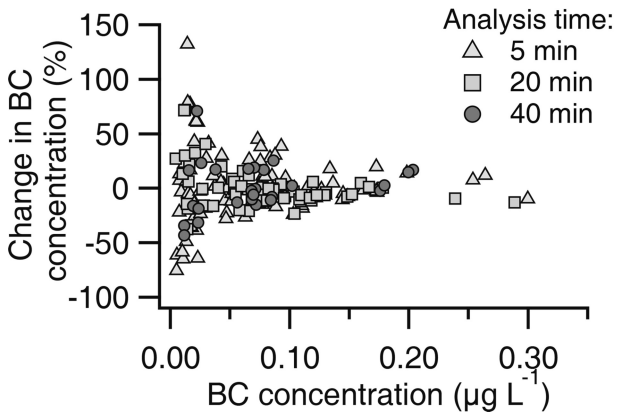

Fig. 4. Changes in BC concentration (y-axis; 1 = 100%) for different BC concentrations (x-axis) for the three different analysis times. Note that when analyzing low-concentration samples (< 0.03 μg L^{-1}), even for long times (40 min) the changes in BC concentrations are significant. Values are relative to the first measurement taken of each sample.

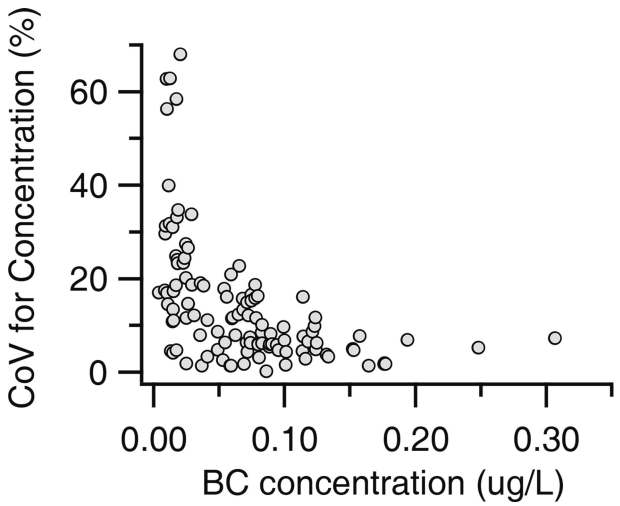

Fig. 5. Coefficient of variation (CoV) for the samples analyzed with the CWU SP2 in the reproducibility test. Vertical axis = CoV for concentrations (gray dots).

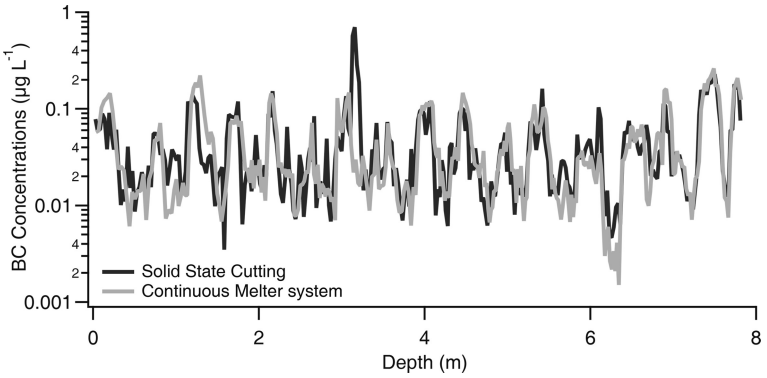

Fig. 6. BC mass concentrations (*y* axis, logarithmic) along the eight meters analyzed.

Table 1. Main results from the comparison between SSC and the CMS. All values are in units of µg L^{-1}. "Geomean" refers to the geometric mean, and 1σ* is the multiplicative standard deviation, representing 68.3% of the variability (Limpert et al., 2001; Bisiaux et al., 2012a).

		Solid-state sampling	Continuous melting system
Total[a]			
	Geomean	0.031	0.029
	1σ* interval	0.013–0.073	0.011–0.076
	Lowest/highest conc.	0.003/0.701	0.001/0.262
Wet-season			
	Geomean	0.019	0.016
	1σ* interval	0.011–0.032	0.008–0.027
	Lowest/highest	0.003/0.083	0.001/0.071
Dry-season			
	Geomean	0.065	0.074
	1σ* interval	0.029–0.121	0.035–0.128
	Lowest/highest	0.007/0.701	0.014/0.262

[a]All samples from section 1 of the core (surface) down to section 8 (around 8 m deep). Total number for solid-state sampling is 307, and for continuous melting system is 343.

0.701 µg L^{-1}, with a geometric mean of 0.031 µg L^{-1} (n = 307). Concentrations using the CMS ranged from < LOD (0.0015 µg L^{-1}) to 0.262 µg L^{-1}, with a geometric mean of 0.029 µg L^{-1} (n = 343).

Summer/fall averages for both methods were also similar, with differences regarding summer/fall highest values due to concentration peaks in the SSC method that did not alter the mean significantly. Winter geometric means were similar for both methods (CMS = 0.074 µg L^{-1}; SSC = 0.065 µg L^{-1}); the winter maximum showed a pronounced difference owing to an anomalous peak around the depth of 3 m, wherein the discrete sampling two consecutive samples achieved 0.701 µg L^{-1} and 0.568 µg L^{-1}, while the continuous melter gave a maximum of 0.147 µg L^{-1} for the same depth. This almost five-fold difference did not appear anywhere else in the core, probably reflecting contamination in the samples, and thus these two SSC samples are not considered in further interpretations.

Figure 7 shows a dry- versus wet-season comparison for both methods. The results are similar for both methods: summer/fall values remain fairly steady for the entire record; winter/spring concentrations show an initial peak in 1998 and 1999 AD, followed by a low in 2002 and an increasing trend from 2002 to 2014—more visible in the CMS record (but with a weak r^2 of 0.2478, not shown).

Annual rBC fluxes were calculated to account for potential biases in annual rBC concentrations due to changes in snow accumulation rates. Fluxes were calculated by multiplying annual rBC concentrations by the annual snow accumulation. rBC annual concentrations were averaged from SSC and the CMS. Concentrations and fluxes followed a similar pattern, implying low variability in snow accumulation during the study period (Fig. 8).

4.6. *Comparison with other rBC cores in Antarctica*

Table 2 compares our results with other rBC records in Antarctica. East Antarctica cores [NUS0X from Bisiaux et al. (2012a)] present the highest elevations and annual rBC concentrations, but the lowest snow accumulation, in recent times (~1800–2000). The authors found a linear positive correlation between site elevation and rBC concentrations for the NUS07 cores, of 0.025 µg L^{-1} (500 m)$^{-1}$, and hypothes-

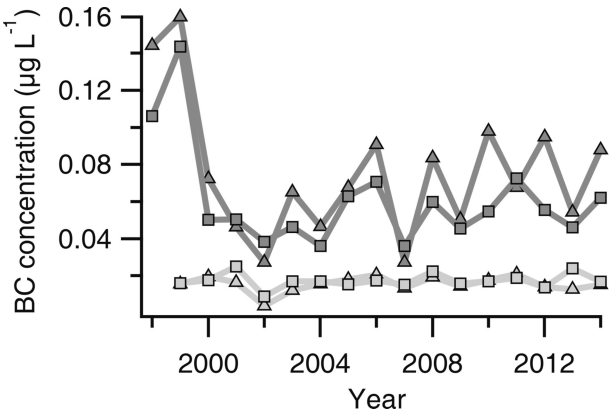

Fig. 7. Comparison between dry- and wet-season average concentrations for both sampling methods: SSC (squares); CMS (triangles). Low-concentration lines are from the wet season; high-concentration lines are from the dry season.

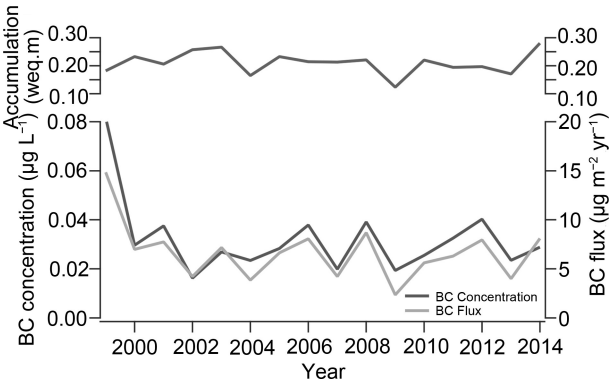

Fig. 8. BC concentrations (SSC and CMS averages) and BC fluxes (SSC and CMS averages) at the site for the first eight sections. Snow accumulation is shown at the top, in units of water equivalent (weq) meters.

ized that rBC inputs to the atmosphere over East Antarctica are not controlled by the intrusion of marine air masses and that transport in the upper troposphere may be more important.

Arienzo et al. (2017) found an even higher annual rBC concentration for the coastal site B40 (0.3 µg L^{-1}), where the flux was calculated to be 20 µg m^{-2} yr^{-1}. As BC is primarily deposited through wet deposition (Flanner et al., 2007), the authors attributed the higher accumulation in coastal areas to the scavenging of most of the BC, with fluxes lowering inland as the accumulation rates decreased.

Arienzo et al. (2017) also found high rBC fluxes for the WAIS ice core for the end of the last glaciation termination (14–12 kBP, 25 µg m^{-2} yr^{-1}) and for the mid-Holocene (12–6 kBP, 45 µg m^{-2} yr^{-1}). The authors attributed the high rBC fluxes in the past to a period of relatively high austral-burning-season and low growing-season insolation.

The WAIS ice core (Bisiaux et al., 2012b; Arienzo et al., 2017) is the closest to TT07 (350 km apart). Although the annual snow accumulation is similar at both sites (0.21 ± 0.04 weq m yr^{-1} for TT07 in this work; 0.20 ± 0.03 weq m^{-1} for WAIS), our annual rBC concentration is less than half that of WAIS during 1850–2001 (0.031 µg L^{-1} for TT07;

Table 2. Coordinates, elevation, period covered and BC information for this study and previous works on Antarctic ice cores. To enable direct comparison, we only list studies that used the SP2.

Source	Core name	Location in Antarctica	Lat./Long.	Elev. (MSL)	Period covered	Annual BC conc. (µg L^{-1})	BC conc. range (2σ)[a]	Annual accum. (weq m yr^{-1})	Annual BC fluxes (µg m^{-2} yr^{-1})	BC flux range (2σ)
This study	TT07	West	79°55'S, 94°21'W	2122	1998–2015	0.029	0.01–0.07	0.21 ± 0.04	6.1	2.6–14.6
Bisiaux et al. (2012b)	WAIS	West	79°46'S, 112°08'W	1766	1850–2001	0.08	0.05–0.12	0.20 ± 0.03	16	9.8–24.4
	Law Dome	East	66°73'S, 112°83'E	1390	1850–2001	0.09	0.05–0.2	0.15 ± 0.03	13.5	7.3–30.6
Arienzo et al. (2017)	WAIS	West	79°46'S, 112°08'W	1766	14–12 kBP	0.12[b]	–	–	25[b]	–
					12–6 kBP	0.2[b]	–	–	45[b]	–
	B40	East	70°0'S, 0°3'E	2911	2.5 k–0 BP	0.3[c]	–	–	20[c]	–
Bisiaux et al. (2012b)	NUS07-1	East	73°43'S, 07°59'E	3174	1800–2006	0.16	0.09 to 0.26	0.05±0.02	8.3	4.6 to 14.2
	NUS07-2		76°04'S, 22°28'E	3582	1800–1993	0.12	0.07–0.19	0.03 ± 0.01	3.9	2.5–6.2
	NUS07-5		78°39'S, 35°38'E	3619	1800–1989	0.14	0.08–0.26	0.02 ± 0.01	3.4	1.8–6.3
	NUS07-7		82°49'S, 54°53'E	3725	1800–2008	0.18	0.12–0.27	0.02 ± 0.01	5.3	3.5–8.0
	NUS08-4		82°49'S, 18°54'E	2552	1800–2004	0.1	0.06–0.18	0.04 ± 0.01	3.7	2.1–6.9
	NUS08-5		82°38'S, 17°52'E	2544	1800–1993	0.11	0.07–0.18	0.03 ± 0.01	3.9	2.2–6.5

[a] Multiplicative standard deviation representing 95.5% of the confidence interval; [b] 50-year average, not annual; [c] 7-years media, not annual

0.08 μg L^{-1} for WAIS). The rBC flux is also lower (6.1 μg m^{-2} yr^{-1} for TT07; 16 μg m^{-2} yr^{-1} for WAIS), although we acknowledge there is not a large temporal overlap between the cores (three years, 1998–2001).

5. Conclusions

This study shows that the CMS with discrete sampling is a faster and more reliable way of analyzing low-dust content samples compared with SSC, despite samples sitting in the liquid state for a longer period of time (maximum of 1 h for SSC versus 2 h for the CMS). A long sample waiting-time in the liquid state is normally not recommended because of the possible changes in rBC concentrations caused by particle adhesion to the vial walls and the agglomeration of particles outside the SP2 detection range (Wendl et al., 2014). However, in this work, the longer time did not reflect any significant changes in rBC concentrations. The CMS record was smoother than the SSC record, probably due to the reduced handling of the snow and firn core during sub-sampling. SSC, though, needs much less volume than the CMS, which could be an advantage when working with limited resources (samples). A Wilcoxon–Mann–Whitney test indicated there to be no statistical difference between the results of the different methods at $p = 0.01$.

The record for these first 8 m of the snow and firn core shows a well-defined seasonal signal, with high rBC concentrations during the dry season (austral winter/spring) and low concentrations during the wet season (austral summer/fall). Both methods were able to identify these variations in rBC.

The TT07 core showed an annual rBC concentration below those of all other rBC cores in Antarctica referenced in this work, and fluxes similar to high-elevation East Antarctica ice cores (Bisiaux et al., 2012a).

Further studies addressing airmass trajectories are necessary to understand this. Arienzo et al. (2017) related the BC input to the WAIS core site to the intrusion of marine air masses, in which case coastal areas should have higher BC concentrations. Bisiaux et al. (2012a) suggested that transport in the upper troposphere may be more important in East Antarctica, in which case higher-elevation sites would show higher BC concentrations. As the TT07 site is located at higher elevation than the WAIS core (2122 MSL versus 1766 MSL, respectively), but has lower rBC concentrations and fluxes than WAIS, we postulate that the deposition of BC at the site is more related to marine air masses than to upper-tropospheric transport.

Acknowledgements. This research is part of the Brazilian Antarctic Program (PROANTAR) and was financed with funds from the Brazilian National Council for Scientific and Technological Development (CNPq) Split Fellowship Program (Grant No. 200386/2018-2) and from the CNPq projects 465680/2014-3 and 442761/2018-0. We thank the Centro Polar e Climático (CPC/UFRGS) and the Department of Geological Sciences (CWU) faculty and staff for their support of this work. We also thank the anonymous reviewers for their comments and suggestions, as well as the *Advances in Atmospheric Sciences* team.

Electronic supplementary material: Supplementary material is available in the online version of this article at https://doi.org/10.1007/s00376-019-9124-8.

REFERENCES

Andela, N., and Coauthors, 2017: A human-driven decline in global burned area. *Science*, **356**, 1356–1362, https://doi.org/10.1126/science.aal4108.

Arienzo, M. M., J. R. McConnell, L. N. Murphy, N. Chellman, S. Das, S. Kipfstuhl, and R. Mulvaney, 2017: Holocene black carbon in Antarctica paralleled Southern Hemisphere climate. *J. Geophys. Res.*, **122**, 6713–6728, https://doi.org/10.1002/2017JD026599.

Bice, K., and Coauthors, 2009: Black carbon: A review and policy recommendations. Woodrow Wilson School of Policy & International Affairs. [Available online at http://www.wws.princeton.edu/research/PWReports/F08/wws591e.pdf]

Bisiaux, M. M., R. Edwards, J. R. McConnell, M. R. Albert, H. Anschütz, T. A. Neumann, E. Isaksson, and J. E. Penner, 2012a: Variability of black carbon deposition to the East Antarctic Plateau, 1800–2000 AD. *Atmospheric Chemistry and Physics*, **12**, 3799–3808, https://doi.org/10.5194/acp-12-3799-2012.

Bisiaux, M. M., and Coauthors, 2012b: Changes in black carbon deposition to Antarctica from two high-resolution ice core records, 1850–2000 AD. *Atmospheric Chemistry and Physics*, **12**, 4107–4115, https://doi.org/10.5194/acp-12-4107-2012.

Bond, T. C., and Coauthors, 2013: Bounding the role of black carbon in the climate system: A scientific assessment. *J. Geophys. Res.*, **118**, 5380–5552, https://doi.org/10.1002/jgrd.50171.

Casey, K. A., S. D. Kaspari, S. M. Skiles, K. Kreutz, and M. J. Handley, 2017: The spectral and chemical measurement of pollutants on snow near South Pole, Antarctica. *J. Geophys. Res.*, **122**, 6592–6610, https://doi.org/10.1002/2016JD026418.

Flanner, M. G., C. S. Zender, J. T. Randerson, and P. J. Rasch, 2007: Present-day climate forcing and response from black carbon in snow. *J. Geophys. Res.*, **112**, D11202, https://doi.org/10.1029/2006JD008003.

Fretwell, P., and Coauthors, 2013: Bedmap2: Improved ice bed, surface and thickness datasets for Antarctica. *The Cryosphere*, **7**, 375–393, https://doi.org/10.5194/tc-7-375-2013.

Hansen, J., and L. Nazarenko, 2004: Soot climate forcing via snow and ice albedos. *Proceedings of the National Academy of Sciences of the United States of America*, **101**, 423–428, https://doi.org/10.1073/pnas.2237157100.

Kaspari, S. D., M. Schwikowski, M. Gysel, M. G. Flanner, S. Kang, S. Hou, and P. A. Mayewski, 2011: Recent increase in black carbon concentrations from a Mt. Everest ice core spanning 1860–2000 AD. *Geophys. Res. Lett.*, **38**, L04703, https://doi.org/10.1029/2010GL046096.

Kaspari, S., S. M. Skiles, I. Delaney, D. Dixon, and T. H. Painter, 2015: Accelerated glacier melt on Snow Dome, Mount Olympus, Washington, USA, due to deposition of black carbon and mineral dust from wildfire. *J. Geophys. Res.*, **120**, 2793–2807, https://doi.org/10.1002/2014JD022676.

Kaspari, S., T. H. Painter, M. Gysel, S. M. Skiles, and M.

Schwikowski, 2014: Seasonal and elevational variations of black carbon and dust in snow and ice in the Solu-Khumbu, Nepal and estimated radiative forcings. *Atmospheric Chemistry and Physics*, **14**, 8089–8103, https://doi.org/10.5194/acp-14-8089-2014.

Katich, J. M., A. E. Perring, and J. P. Schwarz, 2017: Optimized detection of particulates from liquid samples in the aerosol phase: Focus on black carbon. *Aerosol Science and Technology*, **51**, 543–553, https://doi.org/10.1080/02786826.2017.1280597.

Koch, D., T. C. Bond, D. Streets, N. Unger, and G. R. van der Werf, 2007: Global impacts of aerosols from particular source regions and sectors. *J. Geophys. Res.*, **112**, D02205, https://doi.org/10.1029/2005JD007024.

Lauk, C., and K. H. Erb, 2009: Biomass consumed in anthropogenic vegetation fires: Global patterns and processes. *Ecological Economics*, **69**, 301–309, https://doi.org/10.1016/j.ecolecon.2009.07.003.

Legrand, M., and P. Mayewski, 1997: Glaciochemistry of polar ice cores: A review. *Rev. Geophys.*, **35**, 219–243, https://doi.org/10.1029/96RG03527.

Limpert, E., W. A. Stahel, and M. Abbt, 2001: Log-normal distributions across the sciences: Keys and clues: On the charms of statistics, and how mechanical models resembling gambling machines offer a link to a handy way to characterize log-normal distributions, which can provide deeper insight into variability and probability—normal or log-normal: That is the question. *BioScience*, **51**, 341–352, https://doi.org/10.1641/0006-3568(2001)051[0341:lndats]2.0.co;2.

Marlon, J. R., and Coauthors, 2016: Reconstructions of biomass burning from sediment-charcoal records to improve data-model comparisons. *Biogeosciences*, **13**, 3225–3244, https://doi.org/10.5194/bg-13-3225-2016.

Marlon, R. J., and Coauthors, 2008: Climate and human influences on global biomass burning over the past two millennia. *Nature Geoscience*, **1**, 697–702, https://doi.org/10.1038/ngeo313.

Matsuoka, K., A. Skoglund, and G. Roth, 2018: Quantarctica [Data set]. https://doi.org/10.21334/npolar.2018.8516e961.

McConnell, R. J., and Coauthors, 2007: 20th-century industrial black carbon emissions altered arctic climate forcing. *Science*, **317**, 1381–1384, https://doi.org/10.1126/science.1144856.

Mori, T., N. Moteki, S. Ohata, M. Koike, K. Goto-Azuma, Y. Miyazaki, and Y. Kondo, 2016: Improved technique for measuring the size distribution of black carbon particles in liquid water. *Aerosol Science and Technology*, **50**, 242–254, https://doi.org/10.1080/02786826.2016.1147644.

Moteki, N., and Y. Kondo, 2010: Dependence of laser-induced incandescence on physical properties of black carbon aerosols: Measurements and theoretical interpretation. *Aerosol Science and Technology*, **44**, 663–675, https://doi.org/10.1080/02786826.2010.484450.

Olfert, J. S., J. P. R. Symonds, and N. Collings, 2007: The effective density and fractal dimension of particles emitted from a light-duty diesel vehicle with a diesel oxidation catalyst. *Journal of Aerosol Science*, **38**, 69–82, https://doi.org/10.1016/j.jaerosci.2006.10.002.

Osmont, D., M. Sigl, A. Eichler, T. M. Jenk, and M. Schwikowski, 2018a: A Holocene black carbon ice-core record of biomass burning in the Amazon Basin from Illimani, Bolivia. *Climate of the Past*, **15**, 579–592, https://doi.org/10.5194/cp-15-579-2019.

Osmont, D., I. A. Wendl, L. Schmidely, M. Sigl, C. P. Vega, E. Isaksson, and M. Schwikowski, 2018b: An 800-year high-resolution black carbon ice core record from Lomonosovfonna, Svalbard. *Atmospheric Chemistry and Physics Discussions*, https://doi.org/10.5194/acp-2018-244.

Osterberg, C. E., M. J. Handley, S. B. Sneed, P. A. Mayewski, and K. J. Kreutz, 2006: Continuous ice core melter system with discrete sampling for major ion, trace element, and stable isotope analyses. *Environ. Sci. Technol.*, **40**, 3355–3361, https://doi.org/10.1021/es052536w.

Petzold, A., and Coauthors, 2013: Recommendations for reporting black carbon measurements. *Atmospheric Chemistry and Physics*, **13**, 8365–8379, https://doi.org/10.5194/acp-13-8365-2013.

Sand, M., and Coauthors, 2017: Aerosols at the poles: An AeroCom Phase II multi-model evaluation. *Atmospheric Chemistry and Physics*, **17**, 12197–12218, https://doi.org/10.5194/acp-17-12197-2017.

Schwanck, F., J. C. Simões, M. Handley, P. A. Mayewski, R. T. Bernardo, and F. E. Aquino, 2016a: Anomalously high Arsenic concentration in a West Antarctic ice core and its relationship to copper mining in Chile. *Atmos. Environ.*, **125**, 257–264, https://doi.org/10.1016/j.atmosenv.2015.11.027.

Schwanck, F., J. C. Simões, M. Handley, P. A. Mayewski, R. T. Bernardo, and F. E. Aquino, 2016b: Drilling, processing and first results for Mount Johns ice core in West Antarctica Ice Sheet. *Brazilian Journal of Geology*, **46**, 29–40, https://doi.org/10.1590/2317-4889201620150035.

Schwanck, F., J. C. Simões, M. Handley, P. A. Mayewski, J. D. Auger, R. T. Bernardo, and F. E. Aquino, 2017: A 125-year record of climate and chemistry variability at the Pine Island Glacier ice divide, Antarctica. *The Cryosphere*, **11**, 1537–1552, https://doi.org/10.5194/tc-11-1537-2017.

Sigl, M., N. J. Abram, J. Gabrieli, T. M. Jenk, D. Osmont, and M. Schwikowski, 2018: 19th century glacier retreat in the Alps preceded the emergence of industrial black carbon deposition on high-alpine glaciers. *The Cryosphere*, **12**, 3311–3331, https://doi.org/10.5194/tc-12-3311-2018.

Stohl, A., and H. Sodemann, 2010: Characteristics of atmospheric transport into the Antarctic troposphere. *J. Geophys. Res.*, **115**, D02305, https://doi.org/10.1029/2009JD012536.

Tao, G. H., R. Yamada, Y. Fujikawa, A. Kudo, J. Zheng, D. A. Fisher, and R. M. Koerner, 2001: Determination of trace amounts of heavy metals in arctic ice core samples using inductively coupled plasma mass spectrometry. *Talanta*, **55**, 765–772, https://doi.org/10.1016/S0039-9140(01)00509-4.

Wang, Z., J. Chappellaz, K. Park, and J. E. Mak, 2010: Large variations in southern hemisphere biomass burning during the last 650 years. *Science*, **330**, 1663–1666, https://doi.org/10.1126/science.1197257.

Wendl, I. A., J. A. Menking, R. Färber, M. Gysel, S. D. Kaspari, M. J. G. Laborde, and M. Schwikowski, 2014: Optimized method for black carbon analysis in ice and snow using the Single Particle Soot Photometer. *Atmospheric Measurement Techniques Discussions*, **7**, 3075–3111, https://doi.org/10.5194/amtd-7-3075-2014.

Winstrup, M., and Coauthors, 2017: A 2700-year annual timescale and accumulation history for an ice core from Roosevelt Island, West Antarctica. *Climate of the Past Discussions*, https://doi.org/10.5194/cp-2017-101.